Nanomechanics on FGF-2 and heparin reveal slip bond characteristics with pH dependency

Semih Sevim[a], Sevil Ozer[a], Gabriel Jones[b], Joel Wurzel[b], Luying Feng[a], Arielle Fakhraee[c], Naveen Shamsudhin[d], Olgaç Ergeneman[d], Eva Pellicer[e],, Jordi Sort[e,f], Salvador Pané[d], Bradley J. Nelson[d], Hamdi Torun[a]**, Tessa Lühmann[b]**

[a]Department of Electrical and Electronics Engineering, Bogazici University, Bebek 34342 Istanbul, Turkey

[b]Institute of Pharmacy and Food Chemistry, University of Würzburg, Am Hubland, 97074, Würzburg, Germany

[c]Aeon Scientific AG, Schlieren, Rütistrasse 12, 8952, Zurich, Switzerland

[d]Multi Scale Robotics Lab, Institute of Robotics and Intelligent Systems, ETH Zurich, Tannenstrasse 3, 8092, Zurich, Switzerland

[e]Departament de Física, Facultat de Ciències, Universitat Autònoma de Barcelona, Torre C5 par-2, 08193 Bellaterra, Spain.

[f]Institució Catalana de Recerca i Estudis Avançats (ICREA), Ps. Lluís Companys 23, 08010 Barcelona, Spain.

** Corresponding authors:

hamdi.torun@boun.edu.tr

(Hamdi Torun ORCID ID: ID: 0000-0002-7882-286X)

tessa.luehmann@uni-wuerzburg.de

(Tessa Lühmann ORCID ID: 0000-0001-7552-6435)

Keywords: Extracellular matrix, isothermal titration calorimetry, magnetic actuation, hypoxia, atomic force spectroscopy

Abstract

Fibroblast growth factor 2 (FGF-2) – an important paracrine growth factor – binds electrostatically with low micro-molar affinity to heparan sulphates present on extracellular matrix proteins. A single molecular analysis served as a basis to decipher the nanomechanical mechanism of the interaction between FGF-2 and the heparan sulphate surrogate – heparin – with a modular atomic force microscope (AFM) design combining magnetic actuators with force measurements at the low force regime (10^1 – 10^4 pN/s). Unbinding events between FGF-2–heparin complexes were specific and short-lived. Binding between FGF-2 and heparin had strong slip bond characteristics as demonstrated by a decrease of life-time with tensile force on the complex. Unbinding forces between FGF-2 and heparin were further detailed at different pH as relevant for (patho-) physiological conditions. An acidic pH environment (5.5) modulated FGF-2 – heparin binding as demonstrated by enhanced rupture forces needed to release FGF-2 from heparin-FGF-2 complex as compared to physiological conditions. This study provides a mechanistic and hypothesis driven model on how molecular forces may impact FGF-2 release and storage during tissue remodeling and repair.

Introduction

The extracellular matrix (ECM) is composed of various structural and adhesive biomolecules, forming a dense 3 dimensional (3D) network in tissues and organs. Apart from being an anchorage scaffold for cells, the ECM plays a pivotal role in spatial and temporal coordination of growth factors (GF).[1-2] One prominent example is fibroblast growth factor 2 (FGF-2, basic FGF), binding electrostatically in the low micro-molar range to negatively charged heparan sulphate (HS) polysaccharides [3] [4] (**Figure 1A**). After cellular secretion, FGF-2 is stored in the ECM on HS of proteoglycans such perlecan[5] and agrin[6] as well as on basement membranes of connective tissue.[7] It is for this mechanism that the activity of FGF-2 is linked to ECM remodeling, degradation and turnover.[8] As potent mitogenic growth factor, FGF-2 is spatially and temporarily tightly regulated during embryonal development and in tissue repair[9-10], showing proliferative effects on a large number of cell types derived from mesodermal and ectodermal origin, including fibroblasts, mesenchymal stem cells and endothelial cells.[11]

Cell stimulation requires the formation of a ternary complex composed of FGF-2, FGF-receptor, and HS co-receptor located on the cell surface.[12] Therefore, the interaction of FGF-2 and heparin – a HS surrogate – has been extensively studied based on both energetic (isothermal titration calorimetry; ITC)[3] and kinetic characterization (surface plasmon resonance; SPR).[13] However, these methods do not allow investigations of FGF-2 – heparin complex interaction on the single-molecule level as required for building the force landscape of this interaction. In tissues, the ECM is subject to physiological forces including shear stress of the interstitial fluid[14] and at the same time to contraction forces exerted by surrounded cells.[15] Fibroblastic cells undergo periodic, low force (~ 100 pN) subcellular contractions but with repetitive occurrence, which is increased at higher substrate stiffness or during differentiation.[16-17] These findings suggest that tissue forces

and tissue deformations may be relevant for FGF-2's ECM storage and release as well as for binding on cell surfaces. Apart from these physiological considerations, the interaction is also interesting in light of drug delivering matrices engineered from heparinized materials in tissue repair applications.[18] Elucidating the underlying mechanism of the HS mediated interplay of GF with the ECM might provide new avenues for constructing advanced biomimetic scaffolds.

Atomic force microscopy (AFM) has been successfully applied in various biomolecular measurements at single-molecule levels including receptor/ligand interactions and protein folding/unfolding experiments. We previously reported on a modular AFM design combining magnetic actuators for single-molecule force measurements.[19] We integrated an electromagnet to a custom-built AFM head to enable direct magnetic actuation of cantilevers for better system dynamics. Furthermore, we employed this system to mechanically actuate functionalized micro/nano-particles against stationary cantilevers in a new mode of operation.[20] Keeping the cantilever stationary and decreasing the size of the actuators drastically offered substantial advantages for stability, dynamics and resolution.

In this study, we have performed biomolecular pulling as well as force clamp (single molecule constant force) AFM experiments using the method of microparticle-based magnetic actuators to probe the force landscape of heparin – FGF-2 interaction at the molecular level. We applied these methods to analyze unbinding forces and bond life-times between both interaction partners in a physiological state and at pathophysiological conditions, in which we mimicked a stressed cellular microenvironment by lowering the extracellular pH-value as result of hypoxia (low pO_2 levels) as found in wound sites, inflammation, or cancer.[21-22]

Results

Probability of specific heparin – FGF-2 interactions probed with a magnetically actuated atomic force microscope

Heparin and FGF-2 interactions were studied on a molecular level using a customized AFM setup, combining a piezo actuator together with an electromagnetic manipulation system.[19] Miniaturized magnetic, PEGylated (to reduce non-specific interactions) microparticles were used as secondary actuator for biomolecular force spectroscopy and force clamp experiments, as schematically represented in **Figure 1B.** We covalently immobilized low molecular weight heparin onto amine functionalized particles by NHS/EDC chemistry, whereas FGF-2 was physioadsorped onto the cantilever.

At first, we aimed at analyzing the probability of specific unbinding events between both interaction partners in the described AFM system. The observed probability of bonding ruptures was 29.09 ± 3.11 % (**Figure 2A)**. We optimized the concentration of the interacting molecules for probabilities of events at ~ 30 % to ensure that the majority of the recorded events are by virtue of single-molecular interactions.[23] As controls the interaction between heparin decorated beads and FGF-2 was probed in the presence of a 10-fold excess of NaCl (impairing electrostatic interactions between both binding partners), and the probability of bonding was significantly reduced to 7.04 ± 4.2 %. Furthermore, saturation of the FGF-2 binding epitope with soluble heparin before the analysis resulted in a decrease to 1.96 ± 0.31 % of specific unbinding events, whereas non-specific interactions of FGF-2 with the unmodified magnetic particles were 1.53 ± 0.63 % of all events analyzed. Thus, the binding of the FGF-2 modified AFM cantilever and heparin decorated microparticles is specific and occurs via the heparin binding site of FGF-2.

Unbinding of heparin – FGF-2 under constant loading rates

A representative force curve with 670 pN/s loading rate and with a 60 pN unbinding force to liberate FGF-2 from the FGF-2– heparin complex is presented in **Figure 2B.** The data points labeled with black circles (**Figure 2C)** represents the most probable unbinding forces collected for low loading rates using our magnetic actuation method. Additional sets of biomolecular force measurements were repeated using the piezo actuation capability of our AFM system (red stars, **Figure 2C**) and a commercially available AFM system (blue triangles, **Figure 2C**). Single force spectroscopy histograms of all tested methods at increasing order of loading rates are displayed in **Figures S1–S3**. The unbinding forces for individual loading rates were distributed around a single force level as displayed in **Figures S1–S3**, supporting the observation of single-molecular events. All results using different methods and AFM systems were in a good agreement with each other as analyzed by linear regression (R^2 values were 0.96 (low loading rate) and 0.91 (high loading rate), respectively) (**Figure 2C**). Notably, we were able to decipher the heparin – FGF-2 interaction on a single molecule level using the magnetic actuators in our customized AFM setup at the low force regime ($10^1 – 10^4$ pN/s) in contrast to the commercial AFM or by piezo actuation of the same customized AFM system (**Figure 2C**). The method of magnetic particle actuation offered the required level of stability and resolution to probe the molecular interactions at low force regime, which is relevant in physiological conditions and at cellular force levels. The corresponding Bell's parameters (k_{off} and Δx) for the heparin-FGF-2 complex at low ($10^1 – 10^6$ pN/s) and high ($10^6 – 10^7$ pN/s) loading rates were calculated following the relationships (1) and (2) and are summarized in **Table 1**.

The observation of continuous sequence of linear regimes suggested that there are two energy barriers along the reaction coordinate for the heparin-FGF-2 complex. The k_{off} as determined for the low force regime was 0.62 s^{-1}, whereas the k_{off} value for the high loading rate regime was found

to be ~ 4500-fold higher (**Table 1**). The dissociation constant (k_{off}) for the heparin – FGF-2 interaction has been determined building off SPR analysis (k_{off} = 0.43 ± 1.92*10^{-2} s^{-1})[13] and is in good agreement with our findings at the low force regime.

The crystal structure of FGF-2 molecules indicates that the crystal lattice of a single molecule is approximately 3.5 nm x 3.5 nm x 3.5 nm (pdb file: 1BFB). The calculated value of Δx = 0.42 nm for the first force regime (**Table 1**) is within the geometry of a single FGF-2 molecule and within its binding interphase to heparin (**Figure 1**). The shorter value of Δx for the second force regime reflected the Bell's parameters for higher pulling rates.

All following biomolecular pulling and force clamp experiments were thus conducted with the customized magnetic actuator AFM setup. In conclusion, we have used two different AFM setups and three different actuation methods - including the magnetic actuator - during the pulling experiments at constant loading rates. The results were complementary and agreed well with each other, suggesting that the binding of a heparin functionalized magnetic bead or a heparin modified substrate to the cantilever resulted from the interaction between heparin and FGF-2.

Life-time analysis of single heparin – FGF-2 interactions

As next we elucidated the bond life-time spectrum of single heparin – FGF-2 interactions. Our magnetic bead actuation methodology (**Figure 1B**) was used for force clamp experiments as previously described.[20] We deployed various clamping forces, ranging from 19.6 pN to 172.7 pN to study life-times between FGF-2 and heparin. A representative force clamp curve for 67 pN clamping force is shown in **Figure 3A**, resulting in an overall life-time of 400 ms of the FGF-2 and heparin complex. We analyzed the life-time histograms for each clamping force. A representative life-time histogram together with the associated exponential density fit function for a clamping force of 39 pN with a mean value of the exponential fit function of 350 ms is shown in

Figure 3C. All other life-time histograms in respect to the deployed clamping forces are given in **Figure S4**. We also calculated the cumulative probabilities for the clamping forces as shown in **Figure 3B** for three selected clamping forces, respectively. The cumulative probabilities for each clamping force and the exponential cumulative probability density fit functions together with 95% confidence intervals are shown in **Figure S5**. Inverse life-times and corresponding clamping forces were exponentially plotted (**Figure 3D**), and correlated to the unbinding rate at that specific clamping force. The unbinding rate increased at elevated clamping forces, suggesting that the complex between heparin and FGF-2 is subject to simple slip bond dissociation. This observation is in agreement with the data presented in **Figure 2C** where the strength of the unbinding force increased with the molecular loading rate. As a result of these force clamp measurements, k_{off} and Δx values were calculated using equation (1) resulting in 2.44 s^{-1} and 0.02 nm, respectively.

pH dependency of the heparin – FGF-2 interaction

Hypoxia in tissues acidifies the ECM down to pH 5 - 7.[24] Providing that storage involves electrostatic interactions, local pH changes in the cellular microenvironment might contribute to alterations in GF release pattern. To investigate interactions between heparin and FGF-2 at three different pH-values (acidic: pH 5.5, physiological: pH 7.4, alkaline: pH 8.5) we first used conventional isothermal titration calorimetric measurements[3] in order to record binding affinities as read out for FGF-2 stability and as prerequisite for further force spectroscopic experiments.

Titration curves of low molecular heparin and FGF-2 are shown in **Figure 4A-C**. Dissociation constants (K_D), stochiometries (n) and changes in enthalpies (ΔH) were derived after non-linear fitting of the binding isotherms (**Table 2**). The binding of FGF-2 to heparin was enthalpically dominated and decreased linearly from -12.7 ± 0.5 (kcal/mol) to -15.4 ± 0.5 (kcal/mol), and to -20.2 ± 1.1 (kcal/mol) with elevating pH. The stochiometry remained constant at all tested pH-

values with ~ three molecules of FGF-2 interacting with one molecule of heparin when FGF-2 was presented in excess. We were able to identify single K_D values of ~ 200 nM for all tested pH values (**Table 2**). These are in good agreement with previous measurements using low molecular weight heparin (3000 Da) and FGF-2 in HEPES buffered saline at pH 7.4.[3] Although the binding enthalpy (ΔH) of FGF-2 to heparin was reduced by approximately 18 % at acidic compared to physiological conditions, pH did not affect the equilibrium binding constant K_D and, therefore, not the free enthalpy changes (ΔG) of binding between heparin and FGF-2. Notably, the entropic contributions ($T\Delta S$) of FGF-2 and heparin interaction decreased linearly from -3.8 ± 0.46 (kcal/mol) to -11.4 ± 1.1 (kcal/mol) from acidic to alkaline conditions, respectively.

We then switched to our magnetic actuated AFM-setup and performed biomolecular pulling measurements at the three different pH values as indicated above. We have collected force-curves between heparin and FGF-2 at different loading rates (50 pN/s – 7000 pN/s), at pH 5.5, pH 7.4, and pH 8.5, respectively. All collected force spectroscopy histograms are provided in the SI (**Figures S3, S6, and S7**)**.** The most probable unbinding forces to break FGF-2 – interactions are depicted in **Figure 4D** and these increased linearly with respect to the logarithm of the applied loading rates. In contrast to physiological and alkaline conditions, acidic pH increased then stability as demonstrated by increased unbinding forces to liberate FGF-2 from the binary complex (**Figure 4D** black triangles). Supporting this finding, the k_{off} value of the heparin – FGF-2 complex was reduced by 23 % at acidic pH in comparison to physiological and alkaline conditions (**Table 3**).

Discussion

We detailed the interaction between FGF-2 and heparin at the single-molecular level using AFM-based pulling and force clamp experiments, including assessments at different pH as relevant for (patho-)physiological conditions. Our customized AFM system, employing an electromagnet with magnetic beads as actuators, has been previously shown to enable force spectroscopic measurements between biotin and streptavidin serving as a well-studied high affinity model receptor ligand system at high loading rates (10^3 to 30^3 pN/s).[20] Low affinity interactions – characteristic of the FGF-2 – heparin complex as reported here – required a stable AFM setup with maximum resolution particularly when used at the low loading rate regime (10^1 to 10^2 pN/s). Our setup enabled sensitive biomolecular force measurements as the cantilever is operated away from stationary surfaces, allowing low actuation speeds and decrease of contact forces acting on the interacting biomolecules. We were therefore able to vary the loading rate with more than five-orders of magnitude (**Figure 1C**). Our applied magnetic bead actuation method was advantageous for the force clamp experiments, facilitating the stability of force levels applied to the FGF-2–heparin complex, without the need of active feedback as needed in conventional AFM systems. We demonstrated that the interaction between FGF-2 and heparin was specific (**Figure 2A**) and had slip bond characteristics (as the life time decreased with the clamping force; **Figure 3D**). Life-times of FGF-2–heparin complexes were short-lived with ~ 0.41 s without (as extrapolated) and ~ 0.19 s in the presence of an tensile force (clamping force: 172 pN), suggesting that cells exerting forces in the pN-range on the ECM may modulate FGF-2 binding to the ECM. Through this mechanism the availability of bound pools for FGF-2 may indeed be controlled by surrounding cells with cells pulling at the ECM with increased forces as demonstrated during tissue

remodeling[25] driving FGF-2 release – a paracrine growth factor (GF) being a potent regulator of cell growth and differentiation of primarily cells of mesodermal origin as required for tissue repair. Binding between FGF-2 and heparin is based on electrostatic (residues K135, Q134, N27, R120, K119, K129) interactions, hydrogen bonding and van der Waals forces[26], resulting in strong enthalpic contributions during formation of the FGF-2–heparin complex. The determined barrier width $\Delta x = 0.4$ nm for the first force regime (**Table 1**) is about 11 % along the axis of the FGF-2 molecule, assuming the molecule fits in a cubic shape (3.5 nm x 3.5 nm x 3.5 nm).

Our results – as analyzed by ITC - revealed that acidic pH reduced intermolecular interactions (ΔH), whereas the entropic contribution ($T\Delta S$) increased (**Figure 4A–C; Table 2**). For all conditions tested (acidic: pH 5.5, physiological: pH 7.4, alkaline: pH 8.5) the equilibrium dissociation constant K_D and the overall free energy change (ΔG) remained constant. This reciprocal relationship between enthalpy and entropy, resulting in constant free energy levels of the interaction, is known as the enthalpy – entropy (H/S) compensation mechanism.[27] We speculate that the release of hydrogen bonded and trapped water within the binding cavities of FGF-2 and heparin drove the entropy change at acidic conditions, an interaction, strongly impacted by pH. pH dependency of the FGF-2 – heparin interaction was further detailed by biomolecular pulling AFM experiments (**Figure 4D**). Recorded unbinding forces versus loading rates were indistinguishable at physiological and at basic pH-values. In contrast, acidic conditions resulted in a stabilized FGF-2– heparin complex as demonstrated by increased unbinding forces and an overall reduced k_{off} value (**Table 3**). These insights are in line with previous studies, detailing transport of FGF-2 within the pericellular space which did not follow simple diffusion pattern.[28] This is due to the fact that HS are ubiquitous present and in concentrations greatly exceeding FGFs levels in tissues. We speculate that binding of FGF-2 to HS is favored at acidic conditions to form locally

concentrated pools within the ECM (**Figure 4E**). These might contribute in gradient formation as needed to guide cells in angiogenesis or tissue development.[29]

In summary, the insights provided here point to an intriguing self-regulating mechanism based on the observation that (i) acidic pH increases heparin binding of FGF-2 while (ii) strain releases FGF-2 from heparin. Pathophysiological pH decrease as of traumatic ischemia (reducing tissue pH and reflecting process (i) of our experiments) favors FGF-2 binding, thereby replenishment the diseased tissue with this trophic growth factor and directing it from the interstitial space to the sites in need. Once tissue repair has advanced to a state that repairing cells exert strain to the ECM (reflecting process (ii) of our experiments), bound FGF-2 is released, thereby regulating cell growth and differentiation. Certainly, future work is necessary to extrapolate the effects of pH dependency and nanomechanics – as observed on the molecular level here – to another hierarchical level including cells, tissues and, organs in health and disease.

Conclusion

In summary, these data provide first nanomechanical insights into the FGF-2 at the molecular level with a modular AFM system designed for biomolecular experiments. Unbinding events between FGF-2 and heparin were specific with life-times decreasing with tensile force on the bond. Solution pH modulated FGF-2 – heparin binding as demonstrated by enhanced rupture forces at acidic conditions compared to physiological pH with implications for storage and release coordination in the extracellular space. AFM with magnetic bead actuation as demonstrated for protein-ligand interactions here is a convenient tool and may be of general relevance to study intramolecular forces and kinetics at the level of individual molecules.

Acknowledgements

Funding from the FET Open FP7 European project MANAQA (Magnetic Nano Actuators for Quantitative Analysis, 296679) is gratefully acknowledged.

Supplemental information

The Supporting information is available free of charge on the ACS Publications website. Supplemental figures S1–S7 are given in the SI.

Material & Methods

Materials

Carbenicillin disodium, phenylmethanesulfonyl fluoride (PMSF), poly(propylene glycol) (Average Mn ~ 2,000 Da), N-Hydroxysulfosuccinimide sodium salt (Sulfo-NHS), N-(3-Dimethylaminopropyl)-N′-ethylcarbodiimide hydrochloride (EDC) and 2-(N-Morpholino)ethane sulfonic acid hydrate (MES hydrate), bovine serum albumin (BSA) and phosphate buffered saline (PBS) tablets were purchased from Sigma Aldrich (Schnelldorf, Germany). Micromer®-M PEG-NH_2 beads (5 µm) were acquired from micromod Partikeltechnologie (Rostock, Germany). Enoxaparin sodium (low molecular weight heparin) was bought from Sanofi-Aventis (Clexane®, Frankfurt, Germany). Non-conductive Silicon Nitride MLCT-C type cantilever with nominal spring constant of 0.01 N/m–Veeco probes were from Bruker Cooperation (Karlsruhe, Germany). Silicon Nitride PNP-TR type cantilevers with nominal spring constant of 0.08 N/m were from Nanoworld (Neuchatel, Switzerland). All other chemicals used were at least of pharmaceutical grade and were purchased from Sigma-Aldrich (unless noted otherwise).

Expression and purification of murine FGF-2

Murine FGF-2 was subcloned and expressed as described before.[30-31] Briefly, protein expression of the fusionprotein pHisTrx-FGF-2 was induced with 0.2 mM IPTG at OD600 = 0.6 and expression was performed at 30° C at 200 rpm. After 5h cells were harvested by centrifugation and were resuspended in lysis buffer (50 mM Tris-HCl, 150 mM NaCl, 1 mM PMSF, pH 7.5) and solubilized by sonification at 4° C. After centrifugation at 100,000 g for 1h at 4° C (L8-60M Ultracentrifuge, Beckman-Coulter, Brea, CA), the supernatant containing pHisTrx tagged FGF-2 was purified by heparin-sepharose affinity chromatography using an FPLC system (Aekta Purifier, GE, Freiburg, Germany). After dialysis against PBS, supplemented with 1 mM DTT, the

fusionprotein pHisTrx-FGF-2 was cleaved by thrombin (GE, Freiburg, Germany) with a final concentration of 1U thrombin/mg fusionprotein at 4°C overnight. After stopping the reaction with 1 mM PMSF, murine FGF-2 was purified by heparin affinity chromatography. Storage of murine FGF-2 was in PBS supplemented with 3 mM DTT as anti-oxidative agent at -80°C. FGF-2 concentration was determined by UV-absorbance at λ= 280 nm, using an extinction coefficient of 16766 ± 239 ($E^{0.1\%}$ = 0.964) as described.[32]

Decoration of magnetic beads with heparin via EDC/Sulfo-NHS coupling

Magnetic and surface functionalized PEG-NH_2 beads were used to reduce non-specific interactions and to prevent aggregation of the beads during the experiments. 1 mg Enoxaparin was added to the activation buffer (0.1 M MES, 0.5 M NaCl, pH 6.0) containing a tenfold molar excess of EDC and 30 mM Sulfo-NHS as described.[30] The mixture was vortexed and incubated for 15 min at room temperature. After activation, the solution was transferred into concentrated phosphate buffer, containing 0.2 mg PEG-NH_2 beads, to raise the pH above neutral. For at least 2 h the suspension was agitated with a Thermomixer comfort (Eppendorf, Hamburg, Germany) to maintain the particles dispersed in solution. After the coupling reaction the beads were washed several times using PBS with increased ionic strength (0.5 M NaCl) and Milli-Q water.

Physioadsorption of FGF-2 onto cantilevers

MLCT-C and PNP-TR cantilevers were incubated with a FGF-2 droplet with a final concentration of 112.5 µg/mL in PBS for 30 min at room temperature, prior to use. This concentration was chosen to observe probabilities of unbinding events of about 30 %. The spring constant values of all the cantilevers used during the experiments were calibrated using thermal noise method.

Single molecule pulling experiments with magnetic bead actuation

Prior to injection of heparin decorated magnetic beads between the cantilever and a cover slip into the magnetic[33] actuation based AFM system, the cover slip surface was blocked with 50 µL BSA with a final concentration of 40 µg/mL for 30 minutes in order to avoid non-specific adhesions between the functionalized MLCT-C type FGF-2 cantilever and the cover glass. After washing away the excess BSA, 100 µL-droplet of PBS was placed into which the heparin-decorated beads were carefully injected using a micropipette. The concentration of heparin molecules immobilized onto the bead was adjusted for probabilities of unbinding events at about 30 %. Several hundreds of force curves were obtained at different loading rates, ranging from 10^1 to 10^4 pN/s by using the magnetic micro particles as actuators. Values of loading rates on individual force curves were recorded before the specific unbinding events and to avoid the additional effect of PEG-NH_2 polymer on the magnetic bead surface. Three different sets of control experiments were performed to test the specificity of the measured data. The first unbinding control experiment was performed in the presence of 10-fold excess of NaCl in the buffer. The second control experiment was performed after keeping the FGF-2 coated cantilevers inside the heparin solution overnight to saturate the FGF-2 molecules on the cantilever with heparin. In the last control experiment, binding of the FGF-2 coated cantilevers was tested against unmodified blank magnetic beads. Detailed information about the instrument setup and procedures of biomolecular pulling measurements by using the magnetic actuation method are described elsewhere.[19,20]

Single molecule force clamp experiments with magnetic bead actuation

In the force clamp experiments the custom build AFM system was used with electromagnetic actuation. The method of actuating magnetic particles against a stationary cantilever allows for the application of constant force on biomolecules to perform force clamp experiments without any active feedback.[20] The magnetic field and gradient applied on the magnetic particle determine the

force, which can be kept constant by driving the electromagnet with a constant current signal. MLCT type cantilevers and the beads were prepared following the same procedures as described for force pulling experiments. The piezoactuator of the cantilever was used to grab magnetic beads and then constant force was applied on the beads until an unbinding event was observed. The duration of time between the instance when the force was applied and the instance of unbinding, i.e. life-time, was recorded for each condition.

The Bell-Evans model was used for the calculation of the kinetic rate of dissociation (k_{off}) and of the barrier width (Δx).[34] ($k_{off}(F)$) values were determined following the relationships:

$$k_{off}(F) = k_{off}\exp\left(\frac{F}{{k_BT}/{\Delta x}}\right) \quad (1)$$

$$F = \frac{k_BT}{\Delta x}\ln\left(\frac{r_f}{{k_BT}/{\Delta x \cdot k_{off}}}\right) \quad (2)$$

, where k_B is the Boltzmann constant and T is the temperature.

Single molecule pulling experiments with piezo actuation

In addition to the method of magnetic bead actuation, single molecule pulling experiments were also performed using the conventional method of piezo actuation. Two sets of pulling experiments were performed using both the custom-built AFM setup and a commercially available AFM system (Dimension Edge, Bruker, Karlsruhe, Germany). PNP-TR type cantilevers were used for these experiments and the cantilevers were incubated in FGF-2 as described before. These cantilevers were tested against cover slips, which were incubated with heparin with a concentration of 20 µg/mL at room temperature. Then, the excess heparin was washed away and the cover slips were later incubated for 30 minutes with 50 µL of BSA with a concentration of 40 µg/mL, which was washed away after incubation to avoid non-specific interactions. Finally, the experiments were

performed in a 100 µL-droplet of PBS. During the experiments, the piezo actuators of the AFM setups were actuated using triangular waves at various speeds to induce different loading rates ranging from 10^3 to 10^7 pN/s.

Isothermal titration calorimetry

Isothermal titration calorimetry (ITC) experiments were performed on a MicroCal–iTC 200 system (GE healthcare, Munich, Germany). 150 µM heparin dissolved in PBS supplemented with 0.5 mM DTT was titrated in 2 µL steps to 30 µM of FGF-2 in PBS containing 0.5 mM DTT in 4.0 s intervals at different pH values (5.5, 7.4, and 8.5). A constant temperature of 20° C and a stirring speed of 400 rpm were maintained throughout the experiment. A total number of 19 injections were performed. Heats determined in the absence of heparin were subtracted from the titration data before curve fitting. Additionally, an initial 0.4 µL injection was discarded from each dataset to remove the effect of titrant diffusion across the syringe tip during the equilibration process. After the integration of the injection peaks the area (heat exchange per injection) was plotted against the molar ratio of heparin/mFGF-2 assuming a sigmoidal fitting model using Origin® scientific plotting software to calculate the binding enthalpy ΔH and the dissociation constant K_D. The free energy change (ΔG) was calculated from the relationship:

$$\Delta G = RT\ln K_D \tag{3}$$

with R as the universal molar gas constant (1.99 cal $*mol^{-1}K^{-1}$) and T as the absolute temperature. The entropic term ($T\Delta S$) to the free energy was determined following the relationship:

$$T\Delta S = \Delta H - \Delta G \tag{4}$$

Statistics

Data were analyzed to perform one-way ANOVA using the software package MatLab (MathWorks, Natick, Massachusetts, USA). Results were considered statistically significant at $p \leq 0.05$ (*) and results are displayed as mean with standard deviation (SD) unless specified otherwise.

Figure legends

Figure 1: (A) Crystal structure of FGF-2 (grey) interacting with a heparin tetra fragment (blue colored by element). pdb file = 1BFB. (B) Schematic representation of the dually actuated AFM setup, using piezo and/or magnetic actuation method.

Figure 2: (A) Probability of unbinding force for heparin and FGF-2 single molecular interaction and control experiments using magnetic bead actuation method, collective data for the whole range of loading rates from 10^1 to 10^4 pN/s are used. (B) a sample force curve with 670 pN/s loading rate showing 60 pN unbinding force, for the corresponding event from the biomolecular interaction between the heparin labeled magnetic bead and FGF2 functionalized cantilever, (C) Unbinding force versus loading rates graph for heparin and FGF2 pulling experiments using magnetic bead actuation method (black circles), piezo actuation method on custom AFM setup (red stars), and on a commercial AFM system (Dimension Edge, Bruker) (blue triangulars). R^2 values in linear regression for both energy barriers (low and high loading rates) were 0.96 and 0.91, respectively.

Figure 3: (A) A representative force clamp curve with 67 pN clamping force showing 400 ms life-time before unbinding. (B) Cumulative probability density graph of life-times under 19.6 pN (black), 38.9 pN (blue) and 61.6 pN (red) with their corresponding exponential fits. (C) Density histogram versus life time with exponential fitting. (D) Unbinding rate (life time^{-1}) versus clamping force and linear fitting.

Figure 4: Isothermal titration calorimetry curves between heparin and FGF-2 in PBS at a pH of (A) 5.5, (B) 7.4, and (C) 8.5, respectively. (D) The most probable unbinding force versus loading rates graph for heparin and FGF-2 interactions. Each labels represent s the experiments which are carried out in different pH environments i.e. pH 5.5 (black triangles), pH 7.4 (red circles) and pH

8.5 (blue triangles) using magnetic actuation method. (E) Proposed pH dependency model for FGF-2 heparin interaction.

Table: 1: Bell's parameters of heparin FGF-2 interaction at different loading rates regimes.

Table: 2: Thermodynamic parameters of heparin –FGF-2 interaction as analyzed by ITC.

Table: 3: Bell's parameters of heparin FGF-2 interaction at different pH values.

References

1. Taipale, J.; Keski-Oja, J., Growth factors in the extracellular matrix. *FASEB journal : official publication of the Federation of American Societies for Experimental Biology* **1997,** *11* (1), 51-9.
2. Sarrazin, S.; Lamanna, W. C.; Esko, J. D., Heparan sulfate proteoglycans. *Cold Spring Harb Perspect Biol* **2011,** *3* (7).
3. Thompson, L. D.; Pantoliano, M. W.; Springer, B. A., Energetic Characterization of the Basic Fibroblast Growth-Factor Heparin Interaction - Identification of the Heparin-Binding Domain. *Biochemistry-Us* **1994,** *33* (13), 3831-3840.
4. Turnbull, J. E.; Fernig, D. G.; Ke, Y. Q.; Wilkinson, M. C.; Gallagher, J. T., Identification of the Basic Fibroblast Growth-Factor Binding Sequence in Fibroblast Heparan-Sulfate. *J Biol Chem* **1992,** *267* (15), 10337-10341.
5. Deepa, S. S.; Yamada, S.; Zako, M.; Goldberger, O.; Sugahara, K., Chondroitin sulfate chains on syndecan-1 and syndecan-4 from normal murine mammary gland epithelial cells are structurally and functionally distinct and cooperate with heparan sulfate chains to bind growth factors - A novel function to control binding of midkine, pleiotrophin, and basic fibroblast growth factor. *J Biol Chem* **2004,** *279* (36), 37368-37376.
6. Cotman, S. L.; Halfter, W.; Cole, G. J., Identification of extracellular matrix ligands for the heparan sulfate proteoglycan agrin. *Experimental cell research* **1999,** *249* (1), 54-64.
7. Yurchenco, P. D., Basement Membranes: Cell Scaffoldings and Signaling Platforms. *Csh Perspect Biol* **2011,** *3* (2).
8. Gospodarowicz, D.; Cheng, J., Heparin Protects Basic and Acidic Fgf from Inactivation. *J Cell Physiol* **1986,** *128* (3), 475-484.
9. Tomanek, R. J.; Hansen, H. K.; Christensen, L. P., Temporally expressed PDGF and FGF-2 regulate embryonic coronary artery formation and growth. *Arterioscler Thromb Vasc Biol* **2008,** *28* (7), 1237-43.
10. Uebersax, L.; Merkle, H. P.; Meinel, L., Biopolymer-based growth factor delivery for tissue repair: from natural concepts to engineered systems. *Tissue Eng Part B Rev* **2009,** *15* (3), 263-89.
11. Coutu, D. L.; Galipeau, J., Roles of FGF signaling in stem cell self-renewal, senescence and aging. *Aging* **2011,** *3* (10), 920-33.
12. Ornitz, D. M.; Itoh, N., The Fibroblast Growth Factor signaling pathway. *Wiley interdisciplinary reviews. Developmental biology* **2015,** *4* (3), 215-66.
13. Ibrahimi, O. A.; Zhang, F. M.; Hrstka, S. C. L.; Mohammadi, M.; Linhardt, R. J., Kinetic model for FGF, FGFR, and proteoglycan signal transduction complex assembly. *Biochemistry-Us* **2004,** *43* (16), 4724-4730.
14. Swartz, M. A.; Fleury, M. E., Interstitial flow and its effects in soft tissues. *Annu Rev Biomed Eng* **2007,** *9*, 229-256.
15. Paluch, E. K.; Nelson, C. M.; Biais, N.; Fabry, B.; Moeller, J.; Pruitt, B. L.; Wollnik, C.; Kudryasheva, G.; Rehfeldt, F.; Federle, W., Mechanotransduction: use the force(s). *Bmc Biol* **2015,** *13*.
16. Hinz, B., The extracellular matrix and transforming growth factor-beta1: Tale of a strained relationship. *Matrix Biol* **2015,** *47*, 54-65.

17. Legant, W. R.; Miller, J. S.; Blakely, B. L.; Cohen, D. M.; Genin, G. M.; Chen, C. S., Measurement of mechanical tractions exerted by cells in three-dimensional matrices. *Nature methods* **2010,** *7* (12), 969-71.
18. Germershaus, O.; Luhmann, T.; Rybak, J. C.; Ritzer, J.; Meinel, L., Application of natural and semi-synthetic polymers for the delivery of sensitive drugs. *Int Mater Rev* **2015,** *60* (2), 101-130.
19. Sevim, S.; Shamsudhin, N.; Ozer, S.; Feng, L. Y.; Fakhraee, A.; Ergeneman, O.; Pane, S.; Nelson, B. J.; Torun, H., An Atomic Force Microscope with Dual Actuation Capability for Biomolecular Experiments. *Sci Rep-Uk* **2016,** *6*.
20. Sevim, S.; Ozer, S.; Feng, L.; Wurzel, J.; Fakhraee, A.; Shamsudhin, N.; Jang, B.; Alcantara, C.; Ergeneman, O.; Pellicer, E.; Sort, J.; Luhmann, T.; Pane, S.; Nelson, B. J.; Torun, H., Dually actuated atomic force microscope with miniaturized magnetic bead-actuators for single-molecule force measurements. *Nanoscale Horizons* **2016**, *1(6)* 488-495.
21. Eltzschig, H. K.; Carmeliet, P., Hypoxia and inflammation. *The New England journal of medicine* **2011,** *364* (7), 656-65.
22. Chiche, J.; Brahimi-Horn, M. C.; Pouyssegur, J., Tumour hypoxia induces a metabolic shift causing acidosis: a common feature in cancer. *Journal of cellular and molecular medicine* **2010,** *14* (4), 771-94.
23. Tees, D. F. J.; Waugh, R. E.; Hammer, D. A., A microcantilever device to assess the effect of force on the lifetime of selectin-carbohydrate bonds. *Biophysical journal* **2001,** *80* (2), 668-682.
24. Goerges, A. L.; Nugent, M. A., pH regulates vascular endothelial growth factor binding to fibronectin: a mechanism for control of extracellular matrix storage and release. *J Biol Chem* **2004,** *279* (3), 2307-15.
25. Su, F. C.; Wu, C. C.; Chien, S., Review: Roles of Microenvironment and Mechanical Forces in Cell and Tissue Remodeling. *J Med Biol Eng* **2011,** *31* (4), 233-244.
26. Raman, R.; Venkataraman, G.; Ernst, S.; Sasisekharan, V.; Sasisekharan, R., Structural specificity of heparin binding in the fibroblast growth factor family of proteins. *P Natl Acad Sci USA* **2003,** *100* (5), 2357-2362.
27. Breiten, B.; Lockett, M. R.; Sherman, W.; Fujita, S.; Al-Sayah, M.; Lange, H.; Bowers, C. M.; Heroux, A.; Krilov, G.; Whitesides, G. M., Water Networks Contribute to Enthalpy/Entropy Compensation in Protein-Ligand Binding. *J Am Chem Soc* **2013,** *135* (41), 15579-15584.
28. Duchesne, L.; Octeau, V.; Bearon, R. N.; Beckett, A.; Prior, I. A.; Lounis, B.; Fernig, D. G., Transport of fibroblast growth factor 2 in the pericellular matrix is controlled by the spatial distribution of its binding sites in heparan sulfate. *PLoS biology* **2012,** *10* (7), e1001361.
29. Lühmann, T.; Hall, H., Cell Guidance by 3D-Gradients in Hydrogel Matrices: Importance for Biomedical Applications. *Materials* **2009,** *2* (3), 1058.
30. Zhao, H.; Heusler, E.; Jones, G.; Li, L.; Werner, V.; Germershaus, O.; Ritzer, J.; Luehmann, T.; Meinel, L., Decoration of silk fibroin by click chemistry for biomedical application. *Journal of structural biology* **2014,** *186* (3), 420-30.
31. Lühmann, T.; Jones, G.; Gutmann, M.; Rybak, J.-C.; Nickel, J.; Rubini, M.; Meinel, L., Bio-orthogonal Immobilization of Fibroblast Growth Factor 2 for Spatial Controlled Cell Proliferation. *ACS Biomaterials Science & Engineering* **2015,** *1* (9), 740-746.

32. Pantoliano, M. W.; Horlick, R. A.; Springer, B. A.; Vandyk, D. E.; Tobery, T.; Wetmore, D. R.; Lear, J. D.; Nahapetian, A. T.; Bradley, J. D.; Sisk, W. P., Multivalent Ligand-Receptor Binding Interactions in the Fibroblast Growth-Factor System Produce a Cooperative Growth-Factor and Heparin Mechanism for Receptor Dimerization. *Biochemistry-Us* **1994,** *33* (34), 10229-10248.
33. Ibrahimi, O. A.; Zhang, F.; Hrstka, S. C.; Mohammadi, M.; Linhardt, R. J., Kinetic model for FGF, FGFR, and proteoglycan signal transduction complex assembly. *Biochemistry-Us* **2004,** *43* (16), 4724-30.
34. Evans, E.; Ritchie, K., Dynamic strength of molecular adhesion bonds. *Biophysical journal* **1997,** *72* (4), 1541-55.

Table 1:

	Range of loading rate [pN]	**Barrier width, Δx [nm]**	**Kinetic rate of dissociation, k_{off} [s^{-1}]**
Regime 1	$10^1 – 10^6$	0.4244	0.6198
Regime 2	$10^6 – 10^7$	0.0231	2774

Table 2:

	T [K]	**#**	**n**	**K_D [nM]**	**ΔH [kcal/mol]**	**ΔG [kcal/mol]**	**TΔS [kcal/mol]**
pH 5.5	293.15	3	3.41±0.29	221±20	-12.7±0.5	-8.9±0.05	-3.8±0.46
pH 7.4	293.15	4	2.97±0.11	232±5	-15.4±0.5	-8.9±0.01	-6.5±0.48
pH 8.5	293.15	5	3.29±0.42	293±32	-20.2±1.1	-8.8±0.07	-11.4±1.1

Table 3:

pH values	**Range of loading rate [pN]**	**Barrier width, Δx [nm]**	**Kinetic rate of dissociation, k_{off} [s^{-1}]**
pH 5.5	10^1 - 10^4	0.3293	0.5996
pH 7.4	10^1 - 10^4	0.4191	0.7836
pH 8.5	10^1 - 10^4	0.4407	0.7661

Figure 1

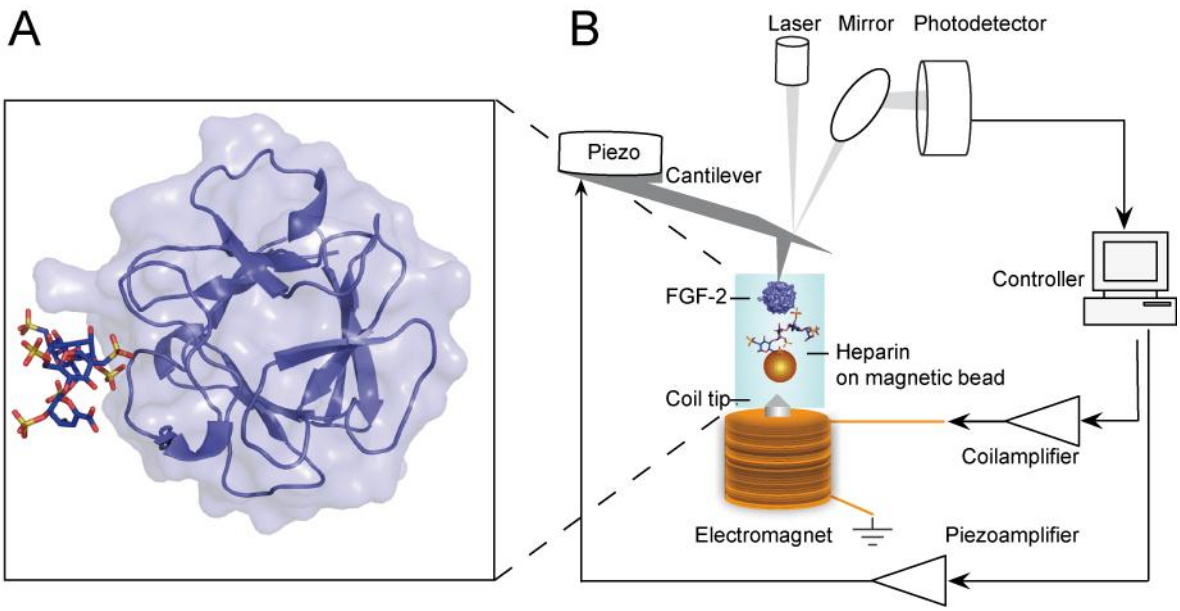
A
B
Laser
Mirror
Photodetector
Piezo
Cantilever
Controller
FGF-2
Heparin
on magnetic bead
Coil tip
Coilamplifier
Electromagnet
Piezoamplifier

Figure 2

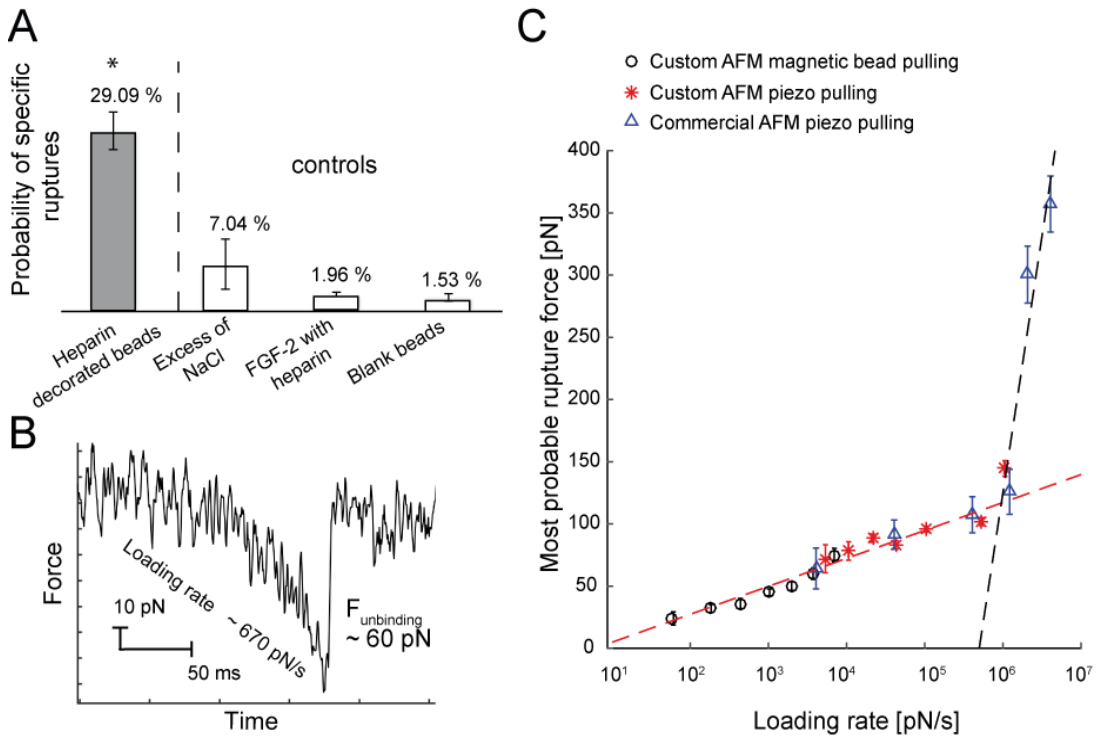
A
Probability of specific ruptures
*
29.09 %
controls
7.04 %
1.96 %
1.53 %
Heparin decorated beads
Excess of NaCl
FGF-2 with heparin
Blank beads
B
Force
Loading rate ~ 670 pN/s
10 pN
50 ms
F unbinding ~ 60 pN
Time
C
Custom AFM magnetic bead pulling
Custom AFM piezo pulling
Commercial AFM piezo pulling
Most probable rupture force [pN]
Loading rate [pN/s]

Figure 3

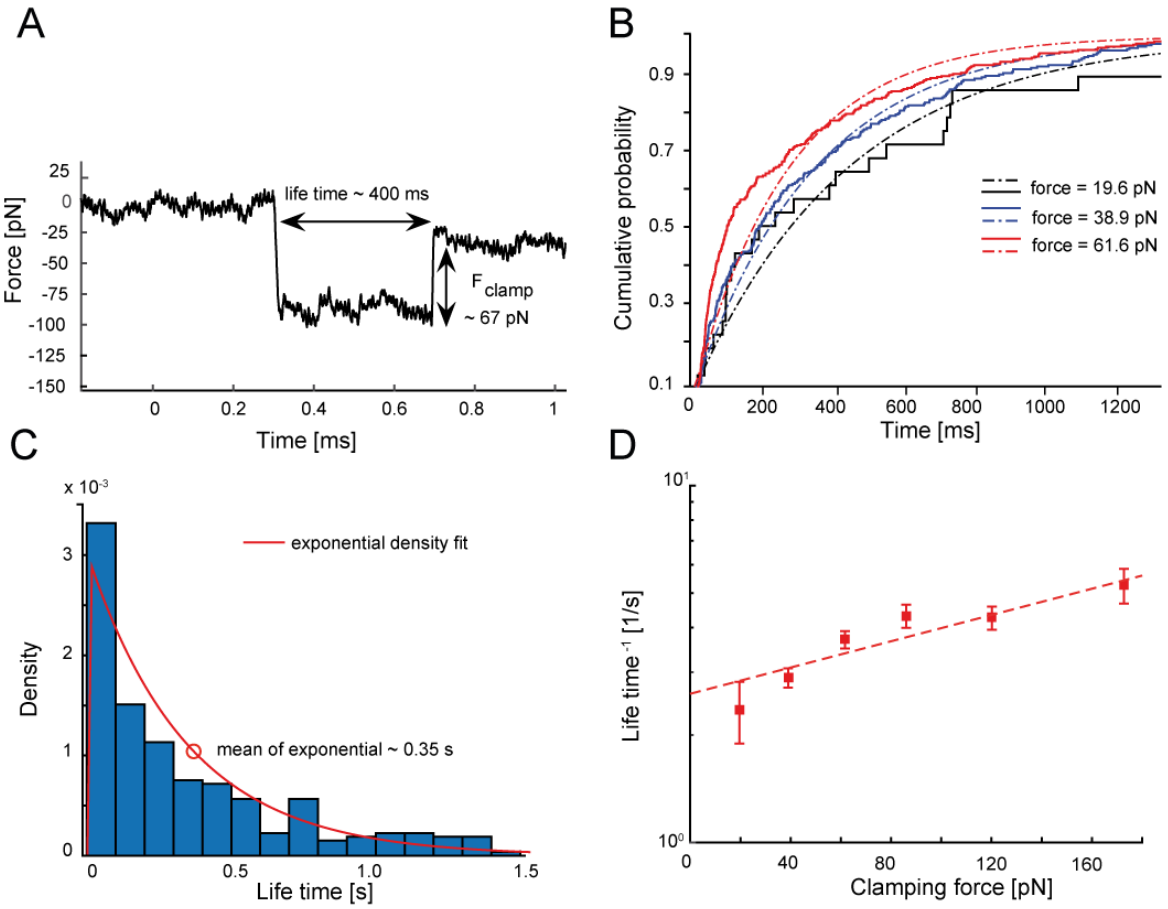
A
Force [pN]
25
0
-25
-50
-75
-100
-125
-150
life time ~ 400 ms
F clamp
~ 67 pN
0
0.2
0.4
0.6
0.8
1
Time [ms]
B
Cumulative probability
0.9
0.7
0.5
0.3
0.1
force = 19.6 pN
force = 38.9 pN
force = 61.6 pN
0
200
400
600
800
1000
1200
Time [ms]
C
x 10-3
Density
3
2
1
0
exponential density fit
mean of exponential ~ 0.35 s
0
0.5
1.0
1.5
Life time [s]
D
Life time-1 [1/s]
101
100
0
40
80
120
160
Clamping force [pN]

Figure 4

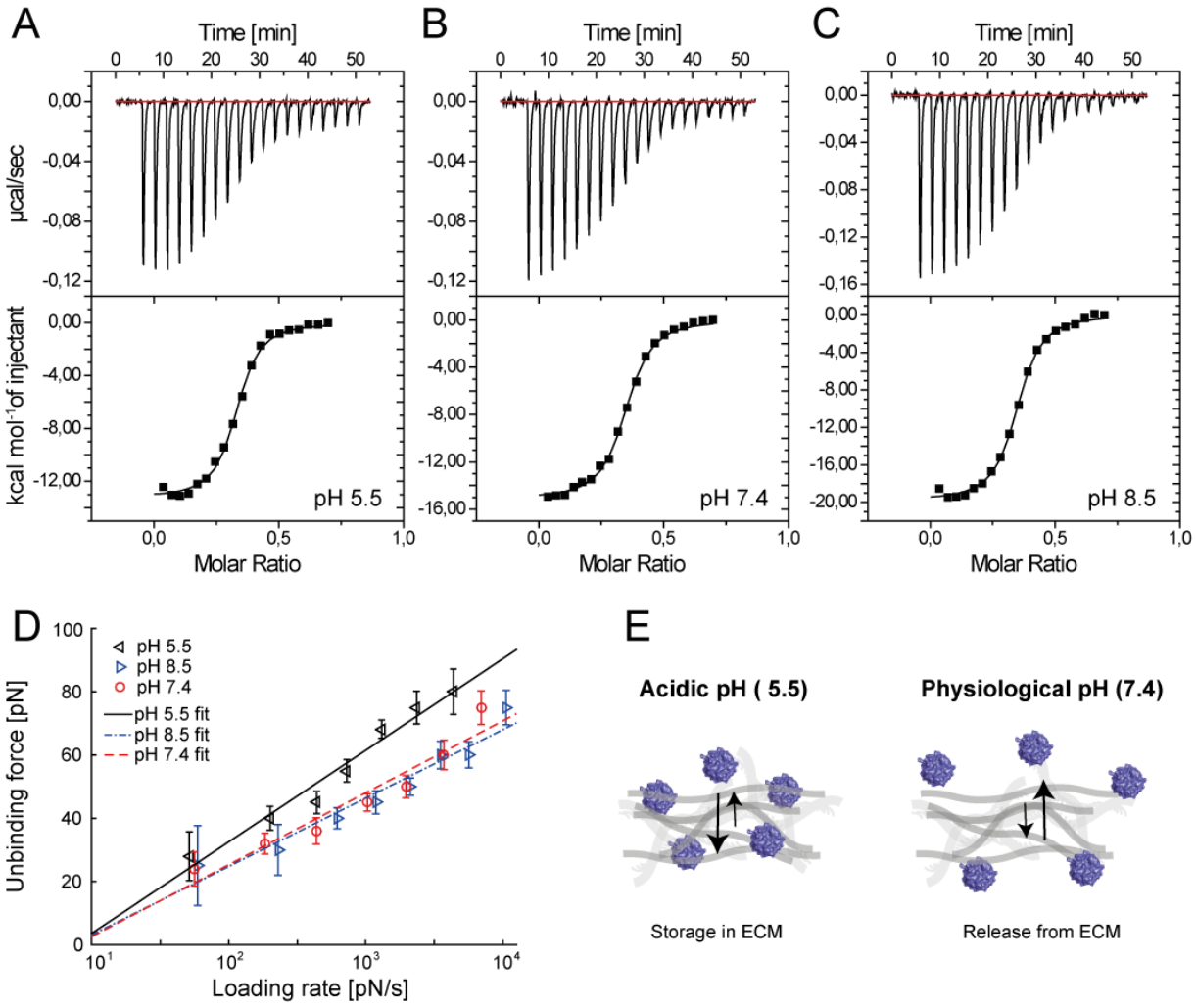
A
B
C
Time [min]
µcal/sec
kcal mol-1 of injectant
pH 5.5
pH 7.4
pH 8.5
Molar Ratio
D
pH 5.5
pH 8.5
pH 7.4
pH 5.5 fit
pH 8.5 fit
pH 7.4 fit
Unbinding force [pN]
Loading rate [pN/s]
E
Acidic pH (5.5)
Physiological pH (7.4)
Storage in ECM
Release from ECM

TABLE OF CONTENTS GRAPHIC

Nanomechanics on FGF-2 and heparin reveal slip bond characteristics with pH dependency

Semih Sevim[a], Sevil Ozer[a], Gabriel Jones[b], Joel Wurzel[b], Luying Feng[a], Arielle Fakhraee[c], Naveen Shamsudhin[d], Olgaç Ergeneman[d], Eva Pellicer[e,], Jordi Sort[e,f], Salvador Pané[d], Bradley J. Nelson[d], Hamdi Torun[a]**, Tessa Lühmann[b]**